

Entanglement production and information scrambling in a noisy spin system

Michael Knap

Department of Physics and Institute for Advanced Study,
Technical University of Munich, 85748 Garching, Germany

(Dated: December 14, 2024)

We study theoretically entanglement and operator growth in a spin system coupled to an environment, which is modeled with classical dephasing noise. Since classical noise retains the unitarity of the time evolution, it does not destroy the quantum information. As a consequence, the main effect of noise is to introduce a new time scale which is proportional to the noise strength, as we obtain from a perturbative treatment. We numerically simulate the noisy spin dynamics and show that entanglement growth and its fluctuations are described by the Kardar-Parisi-Zhang equation. Moreover, we find that the wavefront in the out-of-time ordered correlator (OTOC), which is a measure for the operator growth, propagates linearly with the butterfly velocity and broadens diffusively, with a diffusion constant that is larger than the one of spin transport. A comparison between the entanglement and butterfly velocities unveils that both of them are strongly suppressed with noise, consistent with our perturbative calculation, with the former being smaller than the latter. In our study, we focus on Markovian white noise but also discuss the role of non-Markovian noise.

One of the major challenges in quantum statistical physics is to understand the fundamental principles of the thermalization dynamics in isolated quantum many-body systems [1–3]. An essential part of it is the irreversible growth of quantum information, that is quantified by the growth of the von Neumann entanglement entropy, as a complex quantum many-body system evolves in time [4–8]. Due to the unitarity of the time evolution, quantum information in the initial state is never truly lost. However, it gets scrambled in non-local correlations and is thus not easily accessible in experiments. Operator scrambling can be captured by out-of-time ordered correlators (OTOCs) [9], which have been explored in field theories [10–20], in the semi-classical limit [9, 21–25], and in lattice systems [26–31]. Recently, there has been significant progress in analytically understanding these phenomena in random circuit models, which consist of structureless Haar random gates that are applied stochastically in space and time [7, 32–39]. These quantities are not only of theoretical interest. Due to the unprecedented level of control in synthetic quantum matter, recent experiments were able to measure entanglement entropies [40, 41] and information scrambling [42–44] in complex many-body systems. Since experiments are never truly isolated, it is pertinent to understand how information scrambling and entanglement production is influenced by an environment.

In the present work, we study the entanglement production and information scrambling in a quantum spin system subject to dephasing noise. The effect of the noise is to act as a bath on the spins. We find that in our system the critical exponents for entanglement production are those of the Kardar-Parisi-Zhang (KPZ) equation, which has been originally introduced for stochastic surface growth [45]. This scaling implies that the mean of the entropy grows linearly with time, i.e., we can associate a rate (or ‘velocity’) with the entanglement production. By contrast, the fluctuations scale with a nontrivial powerlaw exponent, see Fig. 1, consistent with results obtained from random unitary circuits [7, 8]. We furthermore, calculate the out-of-time ordered correlator (OTOC) of the quantum

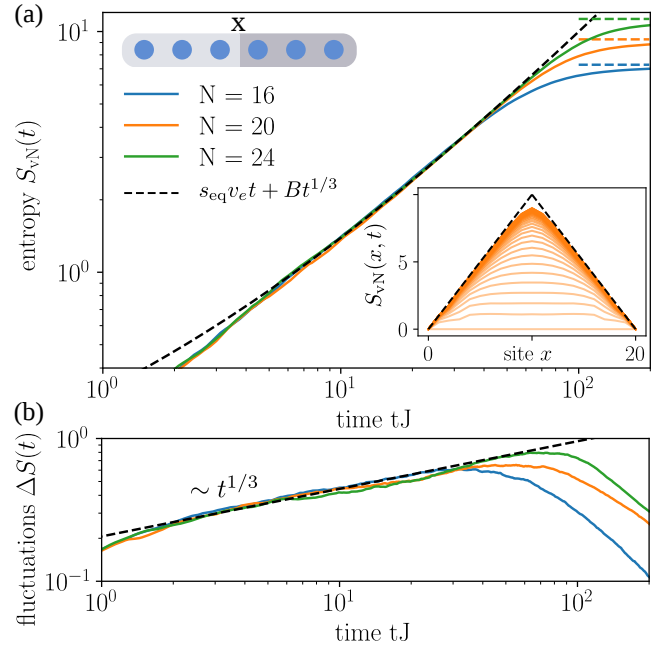


FIG. 1. Entanglement production in a noisy spin chain. We compute the von Neumann entanglement entropy for a Heisenberg chain with N spins starting with initial unentangled product states. In the due course of the dynamics the spins are subjected to dephasing noise of strength $\Lambda = 3\sqrt{J}$. The entanglement cut is chosen to separate the system into two equal halves. (a) The von Neumann entanglement entropy obeys a KPZ scaling with a strong sublinear power-law correction $S_{vN} = s_{eq} v_e t + B t^{1/3}$, dashed line. Inset: The entanglement growth for cuts at different positions x (later times are indicated by more intense colors). (b) As a consequence of the KPZ scaling, the entanglement fluctuations also scale as a powerlaw with exponent $1/3$. At late times the entanglement starts to saturate and hence the power law scaling in the fluctuations breaks down as well.

spins and find that the wavefront of the OTOC can be captured by a biased random walk, i.e., it propagates ballistically with the butterfly velocity and spreads diffusively in time, similarly to the OTOC in random circuit models [32, 35]. Yet, in con-

trast to such random circuits, where gates are applied sequentially at discrete time steps, our model is defined in continuous time. Therefore, in our system we can only define a butterfly velocity but no light-cone velocity. In the strong noise limit, we find that both the entanglement dynamics and the operator scrambling is governed by an effective timescale which is proportional to the noise strength. As a consequence, both the entanglement and the butterfly velocity depend strongly on the noise. Furthermore, the former is strictly smaller than the latter.

As our work was nearing completion two related studies on operator growth in noisy systems appeared [46, 47]. Our work differs from Ref. 46 in that it also considers coherent dynamics and from Ref. 47 in that our work does not necessarily rely on the Markovian white noise limit.

A noisy spin system.—We consider a Heisenberg spin chain, subjected to time dependent noise, as described by

$$\hat{H}_t = -J \sum_j [\vec{S}_j \cdot \vec{S}_{j+1} + \frac{\delta}{2} (S_j^+ S_{j+2}^- + \text{h.c.})] + \sum_j \xi_j(t) \hat{S}_j^z, \quad (1)$$

where we explicitly denote the time dependence of the Hamiltonian by a subscript t . In our model, J is the strength of the Heisenberg coupling of neighboring spins, δ characterizes the next-to-nearest neighbor flip-flop processes, which we introduce to break the integrability of the Heisenberg model, and $\xi_j(t)$ is white noise characterized by a strength Λ (with units of $(\text{energy})^{1/2}$), i.e.,

$$\langle \xi_i(t) \xi_j(t') \rangle = \Lambda^2 \delta(t - t') \delta_{ij}. \quad (2)$$

However, in general, also correlated, non-Markovian noise may be considered by introducing a finite noise correlation time, see e.g. Ref. 48 and 49. We will be interested in how the entanglement production and the spreading of operators changes as a function of the noise strength Λ .

When averaging over all noise trajectories this model can for white noise be mapped onto a Lindblad master equation with jump operators that are given by \hat{S}_j^z [50]:

$$\frac{\partial \hat{\rho}}{\partial t} = \mathcal{L} \hat{\rho} \equiv -i[\hat{H}, \hat{\rho}] + \Lambda^2 \sum_j [\hat{S}_j^z \hat{\rho} \hat{S}_j^z - \frac{1}{4} \hat{\rho}], \quad (3)$$

where \mathcal{L} is the Lindblad superoperator, with a coherent part that generates the Heisenberg time evolution (\hat{H} is the time-independent part of Eq. (1)) and an incoherent part that leads to dephasing.

In the large noise limit $\Lambda^2/J \gg 1$, we show using perturbation theory that both the entanglement and the operator growth are governed by an effective incoherent hopping timescale

$$\tau \sim \Lambda^2/J^2. \quad (4)$$

From that we obtain that diffusion constants, entanglement velocities, and butterfly velocities are parametrically suppressed with noise. Thus only moderately sized systems are required to observe the universal behavior of entanglement production

and operator spreading, which makes it favorable to study this model using exact numerical techniques. We compute the dynamics of our system, fixing $\delta = 0.5$ for various values of the noise strength Λ using exact Krylov time evolution with Eq. (1) and perform the average over noise configurations explicitly.

Entanglement production.—Starting with an unentangled product state $|\psi\rangle$, we evolve our system in time $|\psi(t)\rangle = U_\xi(t)|\psi\rangle$ under the unitary $U_\xi(t) = \mathcal{T} \exp[-i \int_0^t \hat{H}_\tau d\tau]$. At each time step, we bipartition our systems at position x and trace out the subsystem right to the cut (c.f. Fig. 1 (a) top left inset). This leaves us with a density matrix of the left subsystem, $\hat{\rho}_x(t)$. From this density matrix we compute the von Neumann entanglement entropy

$$S_{\text{vN}}(x, t) = -\text{tr}[\hat{\rho}_x(t) \log \hat{\rho}_x(t)]. \quad (5)$$

We choose the basis of the logarithm to be two, so that the maximum entanglement of two spins counts one unit. Time traces of $S_{\text{vN}}(t)$ averaged over several hundreds of noise configurations are shown in Fig. 1 (a) for up to 24 spins. Additional data for other noise strengths and also for Rényi entropies are shown in supplemental material [51].

The entanglement dynamics has been recently computed for analytically tractable models based on random unitary circuits with local Hilbert space dimension q (our case of spin-1/2s corresponds to $q = 2$) [7, 8]. Using the constraints from subadditivity of the von Neumann entropy, the entanglement production has been mapped in the limit of a large local Hilbert space ($q \gg 1$) to a classical growth model which obeys KPZ scaling

$$S_{\text{vN}}(t) = s_{\text{eq}} v_e t + B t^{1/3}, \quad (6)$$

where the first term signals linear growth of the entanglement and the second term is a sublinear correction with a nontrivial power law determined from the KPZ solution [52, 53]. We can interpret the leading linear entanglement growth also as velocity v_e by noting that the entanglement between two consecutive sites in space is the equilibrium entropy s_{eq} in the steady state. A noisy system approaches infinite temperature at late times, hence $s_{\text{eq}} = \log(2) = 1$ (since we measure the logarithm in basis two). Our entanglement production data Fig. 1 (a) is consistent with this form with a rather large prefactor B of the sublinear term which increases relatively to the entanglement growth with noise strength [51].

In the inset of Fig. 1 (a), we show the entanglement entropy for different cuts in space at position x . At early times the average of the entanglement entropy grows uniformly for all cuts, whereas it saturates to the pyramid shaped maximal entanglement (dashed lines) at late times. A consequence of the KPZ scaling of the entanglement entropy is that the entanglement fluctuations in time $\Delta S(x, t) = [(\langle S_{\text{vN}}(t) \rangle - \langle S_{\text{vN}}(x, t) \rangle)^2]^{1/2}$ scale with a nontrivial powerlaw with exponent $1/3$, see Fig. 1 (b); here $\langle \cdot \rangle$ represents both an average over noise trajectories and initial product states. At late times this scaling breaks down because the entanglement saturates

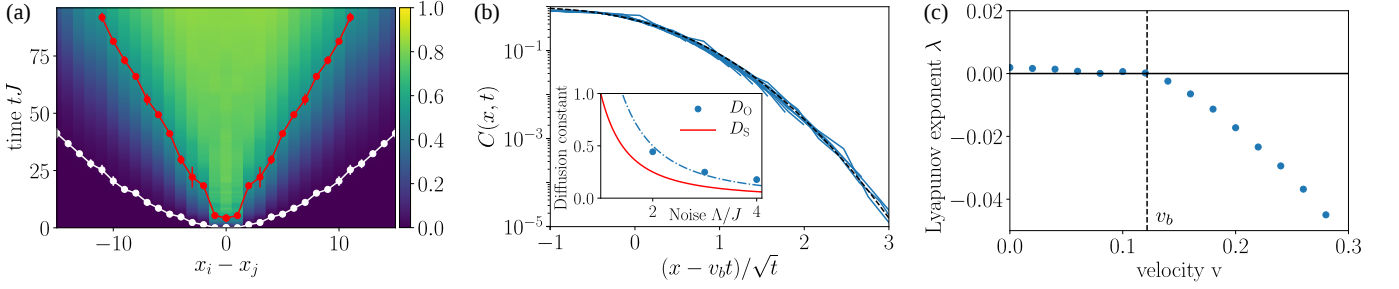


FIG. 2. **Operator scrambling.** We calculate the out-of-time ordered correlator (OTOC) $C(x_i - x_j, t)$ for noise strength $\Lambda = 3\sqrt{J}$. (a) A contour plot of the OTOC is shown in addition to the contour line at which the OTOC takes half (red curve) and one percent (white curve) of its saturation value. Errorbars indicate the standard error of the mean. The slope of the linear red curve defines the inverse butterfly velocity v_b . (b) Scaling collapse over five orders of magnitude of the diffusively broadening right wavefront of the OTOC, which moves with the butterfly velocity $+v_b$. The inset shows the spin diffusion constant D_S , red line, and the diffusion constant of the wavefront D_O . Both diffusion constants scale as $1/\Lambda^2$. (c) The velocity dependent Lyapunov exponent $\lambda(v)$, blue dots, becomes negative at the butterfly velocity v_b .

to a finite value. Our data also confirms the KPZ exponent of $1/2$ for spatial fluctuations of the entanglement entropy (not shown).

Strong noise limit.—The strong noise limit admits a perturbative treatment. We separate the Lindbladian \mathcal{L} , Eq. (3), into the coherent contribution $\mathcal{L}_1\hat{\rho} = -i[\hat{H}, \hat{\rho}]$ and the incoherent contribution $\mathcal{L}_0\hat{\rho} = \sum_j [\hat{S}_j^z \hat{\rho} \hat{S}_j^z - \frac{1}{4}\hat{\rho}]$. In the strong noise limit, we calculate the effects of \mathcal{L}_1 perturbatively. The steady states of the unperturbed (dissipative) term \mathcal{L}_0 are of the form $|s\rangle\langle s|$, where s is a string of spin states in the basis of \hat{S}^z . All of these states have eigenvalue $\lambda_0 = 0$. We can now employ second-order perturbation theory to obtain an effective Lindblad operator

$$\mathcal{L}_{\text{eff}} = \hat{\mathcal{P}} \mathcal{L}_1 \frac{1}{\lambda_0 - \mathcal{L}_0} \mathcal{L}_1 \hat{\mathcal{P}} \quad (7)$$

where $\hat{\mathcal{P}}$ projects onto the subspace of spanned by the eigenstates of \mathcal{L}_0 [54, 55]. In the strong noise limit, we use \mathcal{L}_{eff} to predict the dissipative dynamics.

We will first study time-ordered correlation functions. In our model the total spin $\sum_i \hat{S}_i^z$ is conserved. Hence, long wavelength excitations of such conserved operators follow hydrodynamics, which manifests as a diffusive mode at long wavelengths $\omega(k) = -iD_S k^2 + \dots$, where the dots represent corrections that are of higher order in k [56]. Writing down the equation of motion for \hat{S}_k^z (by replacing $\hat{\rho}$ with \hat{S}_k^z and \hat{H} with $-\hat{H}$ in Eq. (3)) and expanding around small momenta, one obtains the spin diffusion constant [57, 58]

$$D_S = (1 + 4\delta^2) \frac{J^2}{2\Lambda^2}. \quad (8)$$

Hence in the noisy spin system transport is diffusive with the diffusion constant being reduced with increasing noise strength [58, 59]. In the strong noise limit, this relation also holds for arbitrary anisotropies in the $S_j^z S_{j+1}^z$ term of the Heisenberg model.

In our system transport is diffusive, however, operator and entanglement growth is ballistic because of the interac-

tions [5, 26]. Using this perturbative approach, we can moreover compute the timescale that limits the rate of entanglement production and the spreading of the operators (see also Ref. 47). To this end, we consider a Lindblad equation for the operator $\hat{\rho} \otimes \hat{\rho}$ on an extended product space. From $\hat{\rho} \otimes \hat{\rho}$ we obtain the purity of a subsystem by summing over the proper indices, $\langle \rho_x^2(t) \rangle = \langle \sum_{ij} [\rho_x(t)]_{ij} \otimes [\rho_x(t)]_{ji} \rangle$, where the first and second density matrix come from the left and right product space of $\hat{\rho} \otimes \hat{\rho}$ and as before $\hat{\rho}_x$ is the reduced density matrix with spins located at positions right to x are traced out. The entanglement of the purity $S_p = -\log(\langle \rho_x^2(t) \rangle)$ differs from the second Rényi entropy $S_2 = -\langle \log[\text{tr} \rho_x^2(t)] \rangle$ in the orders of the average. However, we find that both quantities behave similarly, see supplemental material [51], which is why we assume the timescale τ obtained from the dynamics of $\hat{\rho} \otimes \hat{\rho}$ governs generally the entropy growth. In a related way, the OTOC can be computed with the time evolved operator copied on the two product spaces [10].

The Lindblad equation for $\hat{\rho} \otimes \hat{\rho}$ is [47, 50]

$$\frac{\partial(\hat{\rho} \otimes \hat{\rho})}{\partial t} = -i[\hat{\mathcal{H}}, \hat{\rho} \otimes \hat{\rho}] + \Lambda^2 \sum_j \left(\hat{S}_j^z \hat{\rho} \otimes \hat{\rho} \hat{S}_j^z - \frac{1}{2} [(\hat{S}_j^z)^2 \hat{\rho} \otimes \hat{\rho} - \hat{\rho} \otimes \hat{\rho} (\hat{S}_j^z)^2] \right), \quad (9)$$

where both $\hat{\mathcal{H}} = \hat{H} \otimes \hat{1} + \hat{1} \otimes \hat{H}$ and $\hat{S}_j^z = \hat{S}_j^z \otimes \hat{1} + \hat{1} \otimes \hat{S}_j^z$ act on the extended space. By performing a perturbative analysis [47, 54] (see supplemental material [51]), one obtains an effective Lindblad superoperator $\mathcal{L}_{\text{eff}} = -\frac{1}{\Lambda^2} \hat{\mathcal{P}} \mathcal{L}_1^2$. As a consequence, the effective timescale for transport, operator growth, and entanglement dynamics scale with the noise Λ^2 , and is determined by incoherent hopping processes; see Eq. (4).

Operator scrambling.—The scrambling of information can be characterized by the out-of-time ordered correlator (OTOC) [9–12]

$$C(x_i, t) = -2 \langle [\hat{S}_i^z(t), \hat{S}_0^z(0)]^2 \rangle. \quad (10)$$

We have introduced the factor of two such that the OTOC grows to the maximal value of one. The OTOC, shown for

noise strength $\Lambda = 3\sqrt{J}$ in Fig. 2, spreads linearly in time and exhibits a pronounced wave-front broadening. From the linear spreading at half of its saturation value, we obtain the butterfly velocity v_b (red line) playing the role of a Lieb Robinson velocity [60]. At lower saturation values, the OTOC spreads with a non-trivial power law (white line), which is why we cannot assign a light cone velocity to the operator dynamics in our model (in contrast to random unitary dynamics where the light cone velocity is defined by the rate at which gates are applied). We demonstrate that the wavefront broadens diffusively by rescaling x as $\frac{x-v_b t}{\sqrt{t}}$, see (b) where we find a scaling collapse over five orders of magnitude. Therefore, the wave-front follows a biased random walk distribution. We can moreover, extract the diffusion constant D_O of the wavefront broadening, by fitting the wavefront to the complementary error function, $\text{erfc}[(x - v_b t)/2\sqrt{D_O t}]$, which is the inverse cumulative distribution function of the Gaussian that governs the biased random walk (dashed black line). The diffusion constant D_O is shown in the inset of (b), blue symbols, along with spin diffusion constant D_S from Eq. (8), red line. The operator diffusion is about a factor two larger than spin diffusion constant and also follows a scaling of $1/\Lambda^2$, dashed-dotted blue line, determined by the incoherent hopping time τ in Eq. (4).

Analogously to the analysis of classical chaos [61, 62], we can introduce a velocity dependent Lyapunov exponent $\lambda(v)$ by analyzing the behavior of the OTOC on constant velocity lines (i.e., rays from the origin in Fig. 2(a)) [25, 60]. In classical systems, the OTOC grows exponentially within the light cone, yet due to the finite local Hilbert space in our quantum system, the OTOC saturates to a finite value within the light cone, which is why the Lyapunov exponent must be strictly zero in that regime, see Fig. 2(c). At the butterfly velocity v_b , $\lambda(v)$ departs from zero and becomes negative indicating an exponential suppression of the OTOC. We find that the butterfly velocity defined in that way coincides with the definition we have used before, dashed line (as the contour line of the OTOC where it obtains half of its saturation value).

Entanglement vs. butterfly velocity.—Combining our analysis of the entanglement production and the operator scrambling we compare the two emergent velocities; the entanglement velocity v_e and the butterfly velocity v_b . We find from our numerical results that $v_e < v_b$ for all values of the noise Λ , see Fig. 3. This inequality results from the diffusive wave-front broadening of the OTOC [33]. Since the operator diffusion constant D_O goes to zero with increasing noise, we expect the two velocities to approach each other, as observed in our data. In the strong noise limit, the effective time scale is $\tau \sim \Lambda^2/J^2$. Since the velocities are inversely proportional to time, they scale as $1/\Lambda^2$ for large Λ , see Fig. 3 where the scaling with $1/\Lambda^2$ is indicated as a black dashed line.

Non-Markovian noise.—So far, we have discussed the Markovian white noise limit, in which transport, entanglement, and operator growth are captured by the same incoherent hopping timescale $\tau \sim \Lambda^2/J^2$. We now argue how this timescale gets modified in the non-Markovian limit in

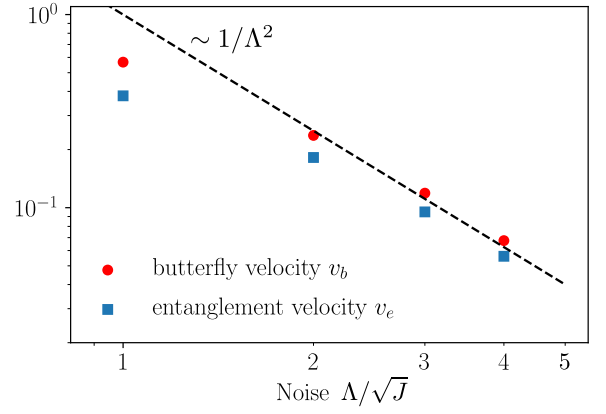


FIG. 3. **Comparison of the entanglement velocity and the butterfly velocity.** The entanglement velocity v_e (blue squares) is strictly smaller than the butterfly velocity v_b (red dots) for all values of the noise Λ , even though they approach each other the stronger the noise is. In the strong noise limit, the velocities are governed by the inverse time scale $\tau^{-1} \sim J^2/\Lambda^2$, which is shown as a black dashed line.

which noise has a finite correlation time. For simplicity we focus on the Ornstein-Uhlenbeck process, $\langle \xi_i(t) \xi_j(0) \rangle = \lambda^2 \exp[-|t|/\sigma] \delta_{ij}$, where σ is the noise correlation time and λ the noise strength which has units of energy. But other forms of noise can be considered as well. The primary mechanism for spreading of charge and information is the incoherent hopping of spins between neighboring sites. Using a Fermi's Golden Rule-type argument, the effective incoherent hopping rate is [48, 49], $\tau^{-1} = 2J^2 |C_\phi(t)|^2$, where $C_\phi(t) = \int_0^\infty e^{-2 \int_0^{t'} (t-t'') \langle \xi(t'') \xi(0) \rangle dt''} dt'$. In the limit of fast noise $\lambda\sigma \ll 1$, $C_\phi(t) \sim 1/(2\lambda^2\sigma)$ and hence

$$\tau_{\text{fast}}^{-1} \sim \frac{J^2}{\lambda^2\sigma} \sim \frac{2J^2}{\int_{-\infty}^{\infty} \langle \xi_i(t) \xi_j(0) \rangle dt}. \quad (11)$$

Evaluating the last expression for white noise, Eq. (2), we obtain our typical noise timescale Eq. (4). This approach generalizes to slow non-Markovian noise $\lambda\sigma \gg 1$, where $C_\phi(t) \sim C_\phi(0) \sim \exp[-\lambda^2 t/2]$. From that we obtain

$$\tau_{\text{slow}}^{-1} \sim \frac{J^2}{\lambda}. \quad (12)$$

Therefore, we find that entanglement and operator growth are scaling differently in the fast and in the slow noise limit. In the latter case the typical time scale is independent of the precise value of the noise correlation time.

Conclusions and Outlook.—In this work, we have studied information scrambling and operator spreading in a noisy spin system, where the noise models the environment. While it might be expected that noise is detrimental for the entanglement and operator growth, classical noise still retains the unitarity of quantum evolution. As a consequence, the main effect of noise is to increase the effective time scale in the system, which scales with the noise strength. As a consequence diffusion constants, butterfly velocities, and entanglement velocities are strongly suppressed with noise. For future

work, it will be interesting to numerically explore our conjecture about entanglement and operator growth timescales in the non-Markovian noise limit. Moreover, an exciting open question is how non-hermitian Lindblad jump operators destroy quantum coherence and what the timescales for such processes are.

Acknowledgments.—M.K. thanks Sarang Gopalakrishnan, Adam Nahum, Frank Pollmann, Tibor Rakovszky, Matteo Scandi, and Herbert Spohn for interesting discussions. This work was supported by the Technical University of Munich - Institute for Advanced Study, funded by the German Excellence Initiative and the European Union FP7 under grant agreement 291763, by the DFG grant No. KN 1254/1-1, and DFG TRR80 (Project F8).

-
- [1] J. M. Deutsch, “Quantum statistical mechanics in a closed system,” *Phys. Rev. A* **43**, 2046–2049 (1991).
 - [2] Mark Srednicki, “Chaos and quantum thermalization,” *Phys. Rev. E* **50**, 888–901 (1994).
 - [3] Marcos Rigol, Vanja Dunjko, and Maxim Olshanii, “Thermalization and its mechanism for generic isolated quantum systems,” *Nature (London)* **452**, 854–858 (2008).
 - [4] Pasquale Calabrese and John Cardy, “Evolution of entanglement entropy in one-dimensional systems,” *J. Stat. Mech.* **2005**, P04010 (2005).
 - [5] Hyungwon Kim and David A. Huse, “Ballistic Spreading of Entanglement in a Diffusive Nonintegrable System,” *Phys. Rev. Lett.* **111**, 127205 (2013).
 - [6] Márk Mezei and Douglas Stanford, “On entanglement spreading in chaotic systems,” [arXiv:1608.05101](#) (2016).
 - [7] Adam Nahum, Jonathan Ruhman, Sagar Vijay, and Jeongwan Haah, “Quantum entanglement growth under random unitary dynamics,” *Phys. Rev. X* **7**, 031016 (2017).
 - [8] Tianci Zhou and Adam Nahum, “Emergent statistical mechanics of entanglement in random unitary circuits,” [arXiv:1804.09737](#) (2018).
 - [9] Larkin A.I. and Ovchinnikov Yu. N., “Quasiclassical method in the theory of superconductivity,” *JETP Lett.* **28**, 1200 (1969).
 - [10] A. Y. Kitaev, “A simple model of quantum holography,” *KITP Program on Entanglement in Strongly-Correlated Quantum Matter* (2015).
 - [11] Stephen H. Shenker and Douglas Stanford, “Black holes and the butterfly effect,” *J. High Energy Phys.* **2014**, 67 (2014).
 - [12] Pavan Hosur, Xiao-Liang Qi, Daniel A. Roberts, and Beni Yoshida, “Chaos in quantum channels,” *J. High Energy Phys.* **2016**, 4 (2016).
 - [13] Joseph Polchinski and Vladimir Rosenhaus, “The spectrum in the Sachdev-Ye-Kitaev model,” *J. High Energy Phys.* **2016**, 1 (2016).
 - [14] Juan Maldacena, Stephen H. Shenker, and Douglas Stanford, “A bound on chaos,” *J. High Energy Phys.* **2016**, 106 (2016).
 - [15] Daniel A. Roberts and Douglas Stanford, “Diagnosing chaos using four-point functions in two-dimensional conformal field theory,” *Phys. Rev. Lett.* **115**, 131603 (2015).
 - [16] Douglas Stanford, “Many-body chaos at weak coupling,” *J. High Energy Phys.* **2016**, 9 (2016).
 - [17] Aavishkar A. Patel, Debanjan Chowdhury, Subir Sachdev, and Brian Swingle, “Quantum butterfly effect in weakly interacting diffusive metals,” *Phys. Rev. X* **7**, 031047 (2017).
 - [18] Yochai Werman, Steven A. Kivelson, and Erez Berg, “Quantum chaos in an electron-phonon bad metal,” [arXiv:1705.07895](#) (2017).
 - [19] Yingfei Gu, Xiao-Liang Qi, and Douglas Stanford, “Local criticality, diffusion and chaos in generalized sachdev-ye-kitaev models,” *J. High Energy Phys.* **2017**, 125 (2017).
 - [20] Shao-Kai Jian and Hong Yao, “Universal properties of many-body quantum chaos at gross-neveu criticality,” [arXiv:1805.12299](#) (2018).
 - [21] Igor L. Aleiner, Lara Faoro, and Lev B. Ioffe, “Microscopic model of quantum butterfly effect: Out-of-time-order correlators and traveling combustion waves,” *Annals of Physics* **375**, 378–406 (2016).
 - [22] Jorge Kurchan, “Quantum bound to chaos and the semiclassical limit,” [arXiv:1612.01278](#) (2016).
 - [23] Efim B. Rozenbaum, Sriram Ganeshan, and Victor Galitski, “Lyapunov exponent and out-of-time-ordered correlator’s growth rate in a chaotic system,” *Phys. Rev. Lett.* **118**, 086801 (2017).
 - [24] Josef Rammensee, Juan-Diego Urbina, and Klaus Richter, “Many-body quantum interference and the saturation of out-of-time-order correlators,” [arXiv:1805.06377](#) (2018).
 - [25] Vedika Khemani, David A. Huse, and Adam Nahum, “Velocity-dependent lyapunov exponents in many-body quantum, semi-classical, and classical chaos,” [arXiv:1803.05902](#) (2018).
 - [26] A. Bohrdt, C. B. Mendl, M. Endres, and M. Knap, “Scrambling and thermalization in a diffusive quantum many-body system,” *New J. Phys.* **19**, 063001 (2017).
 - [27] Xiao Chen, Tianci Zhou, David A. Huse, and Eduardo Fradkin, “Out-of-time-order correlations in many-body localized and thermal phases,” *Annalen der Physik* **529**, 1600332 (2017).
 - [28] David J. Luitz and Yevgeny Bar Lev, “Information propagation in isolated quantum systems,” *Phys. Rev. B* **96**, 020406 (2017).
 - [29] Ivan Kukuljan, Sao Grozdanov, and Toma Prosen, “Weak quantum chaos,” *Phys. Rev. B* **96**, 060301 (2017-08-14).
 - [30] Cheryne Jonay, David A. Huse, and Adam Nahum, “Coarse-grained dynamics of operator and state entanglement,” [arXiv:1803.00089](#) (2018).
 - [31] Silvia Pappalardi, Angelo Russomanno, Bojan Žunkovič, Fernando Iemini, Alessandro Silva, and Rosario Fazio, “Scrambling and entanglement spreading in long-range spin chains,” [arXiv:1806.00022](#) (2018).
 - [32] Adam Nahum, Sagar Vijay, and Jeongwan Haah, “Operator spreading in random unitary circuits,” *Phys. Rev. X* **8**, 021014 (2018).
 - [33] C.W. von Keyserlingk, Tibor Rakovszky, Frank Pollmann, and S.L. Sondhi, “Operator hydrodynamics, OTOCs, and entanglement growth in systems without conservation laws,” *Phys. Rev. X* **8**, 021013 (2018).
 - [34] Vedika Khemani, Ashvin Vishwanath, and D. A. Huse, “Operator spreading and the emergence of dissipation in unitary dynamics with conservation laws,” [arXiv:1710.09835](#) .
 - [35] Tibor Rakovszky, Frank Pollmann, and C. W. von Keyserlingk, “Diffusive hydrodynamics of out-of-time-ordered correlators with charge conservation,” [arXiv:1710.09827](#) (2017).
 - [36] Amos Chan, Andrea De Luca, and J. T. Chalker, “Solution of a minimal model for many-body quantum chaos,” [arXiv:1712.06836](#) (2017).
 - [37] Sarang Gopalakrishnan, “Operator growth and eigenstate entanglement in an interacting integrable floquet system,” [arXiv:1806.04156](#) (2018).
 - [38] Alioscia Hamma, Siddhartha Santra, and Paolo Zanardi,

- “Quantum entanglement in random physical states,” *Phys. Rev. Lett.* **109**, 040502 (2012).
- [39] Winton Brown and Omar Fawzi, “Decoupling with random quantum circuits,” *Commun. Math. Phys.* **340**, 867–900 (2015).
- [40] Rajibul Islam, Ruichao Ma, Philipp M. Preiss, M. Eric Tai, Alexander Lukin, Matthew Rispoli, and Markus Greiner, “Measuring entanglement entropy in a quantum many-body system,” *Nature* **528**, 77–83 (2015).
- [41] Adam M. Kaufman, M. Eric Tai, Alexander Lukin, Matthew Rispoli, Robert Schittko, Philipp M. Preiss, and Markus Greiner, “Quantum thermalization through entanglement in an isolated many-body system,” *Science* **353**, 794–800 (2016).
- [42] Martin Gärttner, Justin G. Bohnet, Arghavan Safavi-Naini, Michael L. Wall, John J. Bollinger, and Ana Maria Rey, “Measuring out-of-time-order correlations and multiple quantum spectra in a trapped-ion quantum magnet,” *Nat. Phys.* **13**, 781–786 (2017).
- [43] Jun Li, Ruihua Fan, Hengyan Wang, Bingtian Ye, Bei Zeng, Hui Zhai, Xinhua Peng, and Jiangfeng Du, “Measuring out-of-time-order correlators on a nuclear magnetic resonance quantum simulator,” *Phys. Rev. X* **7**, 031011 (2017).
- [44] Kevin A. Landsman, Caroline Figgatt, Thomas Schuster, Norbert M. Linke, Beni Yoshida, Norm Y. Yao, and Christopher Monroe, “Verified quantum information scrambling,” *arXiv:1806.02807* (2018).
- [45] Mehran Kardar, Giorgio Parisi, and Yi-Cheng Zhang, “Dynamic scaling of growing interfaces,” *Phys. Rev. Lett.* **56**, 889–892 (1986).
- [46] Shenglong Xu and Brian Swingle, “Locality, quantum fluctuations, and scrambling,” *arXiv:1805.05376* (2018).
- [47] Daniel A. Rowlands and Austen Lamacraft, “Noisy coupled qubits: Operator spreading and the fredrickson-andersen model,” *arXiv:1806.01723* (2018).
- [48] Sarang Gopalakrishnan, K. Ranjibul Islam, and Michael Knap, “Noise-induced subdiffusion in strongly localized quantum systems,” *Phys. Rev. Lett.* **119**, 046601 (2017).
- [49] Ariel Amir, Yoav Lahini, and Hagai B. Perets, “Classical diffusion of a quantum particle in a noisy environment,” *Phys. Rev. E* **79**, 050105 (2009).
- [50] Heinz-Peter Breuer and Francesco Petruccione, *The Theory Of Open Quantum Systems* (Oxford University Press, Oxford, 2002).
- [51] See supplementary online material.
- [52] Michael Prähofer and Herbert Spohn, “Universal distributions for growth processes in 1+1 dimensions and random matrices,” *Phys. Rev. Lett.* **84**, 4882–4885 (2000).
- [53] Michael Prähofer and Herbert Spohn, “Statistical self-similarity of one-dimensional growth processes,” *Physica A (Amsterdam)* **279**, 342–352 (2000).
- [54] Zi Cai and Thomas Barthel, “Algebraic versus exponential decoherence in dissipative many-particle systems,” *Phys. Rev. Lett.* **111**, 150403 (2013).
- [55] Igor Lesanovsky and Juan P. Garrahan, “Kinetic constraints, hierarchical relaxation, and onset of glassiness in strongly interacting and dissipative rydberg gases,” *Phys. Rev. Lett.* **111**, 215305 (2013).
- [56] P. M. Chaikin and T. C. Lubensky, *Principles of Condensed Matter Physics* (Cambridge University Press, Cambridge; New York, USA, 2000).
- [57] Michel Bauer, Denis Bernard, and Tony Jin, “Stochastic dissipative quantum spin chains (i) : Quantum fluctuating discrete hydrodynamics,” *SciPost Physics* **3**, 033 (2017).
- [58] Xizhi Han and Sean A. Hartnoll, “Locality bound for dissipative quantum transport,” *arXiv:1806.01859* (2018).
- [59] Marko Žnidarič, “Dephasing-induced diffusive transport in the anisotropic heisenberg model,” *New J. Phys.* **12**, 043001 (2010).
- [60] Elliott H. Lieb and Derek W. Robinson, “The finite group velocity of quantum spin systems,” *Commun. Math. Phys.* **28**, 251–257 (1972).
- [61] Robert J. Deissler, “One-dimensional strings, random fluctuations, and complex chaotic structures,” *Physics Letters A* **100**, 451–454 (1984).
- [62] Kunihiko Kaneko, “Lyapunov analysis and information flow in coupled map lattices,” *Physica D: Nonlinear Phenomena* **23**, 436–447 (1986).

Supplemental Material: Entanglement production and information scrambling in a noisy spin system

Additional data on the entanglement entropies

Additional data on the growth of the von Neumann entanglement entropy is shown in Fig. S1 (a) for different values of the noise strength Λ and for systems of 20 spins. With increasing noise the entanglement growth gets suppressed. The subleading term B gains weight relatively to the entanglement velocity, inset.

Rényi entropies generalize the von Neumann entropy and are defined as

$$S_n(x, t) = \left\langle \frac{1}{1-n} \log[\text{tr}(\rho_x^n(t))] \right\rangle \quad (\text{S1})$$

In the limit $n \rightarrow 1$, the Rényi entropy reduces to the von Neumann entropy. In Fig. S1 we show the von Neumann entropy along with Rényi entropies with index $n = 2, 4, 8$ for noise strength $\Lambda = 2\sqrt{J}$. The subleading contribution to the entanglement production becomes weaker for increasing Rényi index. In addition the saturation value of the Rényi entropies decreases with Rényi index, see inset in Fig. S1, which is consistent with recent results on random unitary circuit models [8], in which a generalized Page formula for the saturation value has been derived $S_n^{\text{Page}} = \frac{N}{2} \log 2 - \log C_n / (n-1)$, where C_n is the n -th Catalan number. We have also computed the Purity entropy, $S_{\text{Purity}} = \log[\langle \text{tr}(\rho_x^2(t)) \rangle]$, where the trace and the average over noise is exchanged compared to the second Rényi entropy. Both of these entropies are very close to each other.

Strong noise expansion

The effective Lindblad operator for $\hat{\rho}$.—In this section we construct the effective Lindblad superoperator in the strong-noise limit [54]. We separate the Lindblad superoperator into a dissipative part $\mathcal{L}_0 \hat{\rho} = \sum_j [\hat{S}_j^z \hat{\rho} \hat{S}_j^z - \frac{1}{4} \hat{\rho}]$, which dominates for strong noise, and a perturbative, coherent part $\mathcal{L}_1 \hat{\rho} = -i[\hat{H}, \hat{\rho}]$. We construct the effective Lindblad operator by second order perturbation theory $\mathcal{L}_{\text{eff}}^\rho = \hat{\mathcal{P}} \mathcal{L}_1 \frac{1}{\lambda_0 - \mathcal{L}_0} \mathcal{L}_1 \hat{\mathcal{P}}$, Eq. (7).

The steady states of the unperturbed term \mathcal{L}_0 are spin configurations in the z -basis, $|\mathbf{s}\rangle\langle\mathbf{s}|$, as $\mathcal{L}_0 |\mathbf{s}\rangle\langle\mathbf{s}| = \Lambda^2 \sum_j \hat{S}_j^z |\mathbf{s}\rangle\langle\mathbf{s}| \hat{S}_j^z - \frac{1}{4} |\mathbf{s}\rangle\langle\mathbf{s}| = 0$. The perturbation \mathcal{L}_1 generates the coherent time evolution with the Heisenberg Hamiltonian with next-to-nearest neighbor spin exchange $\hat{H} = -J \sum_j [\frac{1}{2} (S_j^+ S_{j+1}^- + S_j^- S_{j+1}^+) + \frac{\delta}{2} (S_j^+ S_{j+2}^- + S_j^- S_{j+2}^+) + S_j^z S_{j+2}^z]$. Since the ferromagnetic

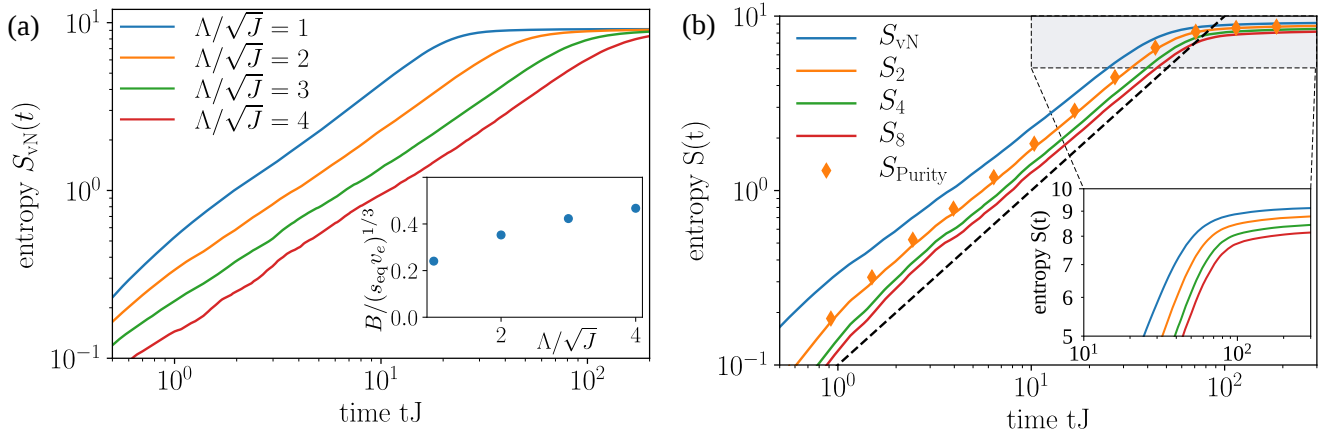


FIG. S1. **von Neumann, Rényi, and purity entanglement entropies.** (a) Entanglement growth for different values of the noise strength Λ in a spin chain of length $N = 20$. Inset: The ratio between the subleading contribution to the entanglement growth and the entanglement growth rate increases with noise. (b) The Rényi entropies S_n are shown for noise strength $\Lambda = 2\sqrt{J}$ along with the von Neumann entropy and the purity entropy. The purity entropy, diamonds, is very close to the second Rényi entropy. The subleading corrections B to the entanglement entropies decreases with the index n of the Rényi entropy. Inset: The saturation value of the entropy decreases with increases Rényi index n .

coupling commutes with $|s\rangle\langle s|$, it does not generate dynamics. The action of \mathcal{L}_0 on the operator product $S_j^+ S_{j+a}^-$ is

$$\begin{aligned}\mathcal{L}_0(S_j^+ S_{j+a}^-) &= \Lambda^2 \sum_i (S_i^z S_j^+ S_{j+a}^- S_i^z - \frac{1}{4} S_j^+ S_{j+a}^-) \\ &= \Lambda^2 (S_j^z S_j^+ S_j^- S_{j+a}^- + S_j^+ S_{j+a}^z S_{j+a}^- S_{j+a}^z - \frac{1}{2} S_j^+ S_{j+a}^-) = -\Lambda^2 S_j^+ S_{j+a}^-\end{aligned}$$

and similarly

$$\mathcal{L}_0(S_j^- S_{j+a}^+) = -\Lambda^2 S_j^- S_{j+a}^+$$

Therefore, we obtain for the effective Lindblad operator [54]

$$\mathcal{L}_{\text{eff}}^\rho = \frac{1}{\Lambda^2} \hat{\mathcal{P}}(\mathcal{L}_1)^2 \hat{\mathcal{P}}. \quad (\text{S2})$$

The effective Lindblad operator for $\hat{\rho} \otimes \hat{\rho}$.—The purity can be calculated by judiciously contracting the indices of $\hat{\rho} \otimes \hat{\rho}$. The OTOC can be obtained in a similar way by time evolving $S_i^z(t) \otimes S_i^z(t)$ and contracting the initial state with $S_0^z(0)$. Therefore, we will analyze the strong coupling limit of the Lindblad equation for $\hat{\rho} \otimes \hat{\rho}$, Eq. (9),

$$\frac{\partial(\hat{\rho} \otimes \hat{\rho})}{\partial t} = -i[\hat{\mathcal{H}}, \hat{\rho} \otimes \hat{\rho}] + \Lambda^2 \sum_j \left(\hat{S}_j^z \hat{\rho} \otimes \hat{\rho} \hat{S}_j^z - \frac{1}{2} [(\hat{S}_j^z)^2 \hat{\rho} \otimes \hat{\rho} - \hat{\rho} \otimes \hat{\rho} (\hat{S}_j^z)^2] \right).$$

Here, $\hat{\mathcal{H}} = \hat{H} \otimes \hat{1} + \hat{1} \otimes \hat{H}$ and $\hat{S}_j^z = \hat{S}_j^z \otimes \hat{1} + \hat{1} \otimes \hat{S}_j^z$ act on the product space. We proceed now similarly to the construction of \mathcal{L}_{eff} for the density matrix by introducing the unperturbed Lindblad operator $\mathcal{L}_0 = \Lambda^2 \sum_j \left(\hat{S}_j^z \hat{\rho} \otimes \hat{\rho} \hat{S}_j^z - \frac{1}{2} [(\hat{S}_j^z)^2 \hat{\rho} \otimes \hat{\rho} - \hat{\rho} \otimes \hat{\rho} (\hat{S}_j^z)^2] \right)$ and the perturbed one $\mathcal{L}_1 = -i[\hat{\mathcal{H}}, \hat{\rho} \otimes \hat{\rho}]$.

First, we find the steady states of \mathcal{L}_0 . By noting that $(\hat{S}_j^z)^2 = 2[\hat{S}_j^z \otimes \hat{S}_j^z + \frac{1}{4}]$, we can read off the following classes of steady states (see also Ref. 47), $|s, \mathbf{u}\rangle\langle s, \mathbf{u}|$ and $|s, \bar{s}\rangle\langle s, \bar{s}|$, where s, \mathbf{u} are configurations of spin-z eigenstates and \bar{s} is the spin flipped configuration of s . Let us calculate the effect of \mathcal{L}_0 on the perturbed states $\mathcal{L}_1|s, \mathbf{u}\rangle\langle s', \mathbf{u}'|$:

$$\mathcal{L}_0(\mathcal{L}_1|s, \mathbf{u}\rangle\langle s', \mathbf{u}'|) = \Lambda^2 \sum_j \left(\hat{S}_j^z \mathcal{L}_1|s, \mathbf{u}\rangle\langle s', \mathbf{u}'| \hat{S}_j^z - \frac{1}{2} [(\hat{S}_j^z)^2 \mathcal{L}_1|s, \mathbf{u}\rangle\langle s', \mathbf{u}'| - \mathcal{L}_1|s, \mathbf{u}\rangle\langle s', \mathbf{u}'| (\hat{S}_j^z)^2] \right)$$

Evaluating this expression for the steady states, $|s, \mathbf{u}\rangle\langle s, \mathbf{u}|$ and $|s, \bar{s}\rangle\langle s, \bar{s}|$ similarly as before, we find that in both cases they have an eigenvalue Λ^2 . Hence, we find in total

$$\mathcal{L}_{\text{eff}}^{\rho \otimes \rho} = -\frac{1}{\Lambda^2} \hat{\mathcal{P}}(\mathcal{L}_1)^2 \hat{\mathcal{P}}. \quad (\text{S3})$$

The scaling with noise is the same as for conventional time ordered expectation values, Eq. (S2). As a consequence, transport, operator scrambling, and entanglement production is in the strong noise limit governed by the same effective scaling with the noise strength, cf. Eq. (4),

$$\tau^{-1} \sim (1 + \delta)^2 \frac{J^2}{\Lambda^2},$$

where the factor $(1 + \delta)^2 J^2$ comes from the nearest and next-to-nearest neighbor in-plane Heisenberg coupling in \mathcal{L}_1 , which is applied twice in Eq. (S3).